

---

**TRAVELING WAVE AMPLIFIER DRIVEN BY A  
LARGE DIAMETER ANNULAR ELECTRON BEAM IN  
A DISK-LOADED STRUCTURE**

**Yue Ying Lau**

**University of Michigan  
Department of Nuclear Engineering and Radiological Sciences  
2355 Bonisteel Blvd.  
Ann Arbor, MI 48109-2104**

**30 October 2015**

**Final Report**

**APPROVED FOR PUBLIC RELEASE; DISTRIBUTION IS UNLIMITED.**



**AIR FORCE RESEARCH LABORATORY  
Directed Energy Directorate  
3550 Aberdeen Ave SE  
AIR FORCE MATERIEL COMMAND  
KIRTLAND AIR FORCE BASE, NM 87117-5776**

---

## NOTICE AND SIGNATURE PAGE

Using Government drawings, specifications, or other data included in this document for any purpose other than Government procurement does not in any way obligate the U.S. Government. The fact that the Government formulated or supplied the drawings, specifications, or other data does not license the holder or any other person or corporation; or convey any rights or permission to manufacture, use, or sell any patented invention that may relate to them.

Qualified requestors may obtain copies of this report from the Defense Technical Information Center (DTIC) (<http://www.dtic.mil>).

AFRL-RD-PS-TR-2015-0041 HAS BEEN REVIEWED AND IS APPROVED FOR PUBLICATION IN ACCORDANCE WITH ASSIGNED DISTRIBUTION STATEMENT.

//MATTHEW DOMONKOS//

---

MATTHEW DOMONKOS, DR-IV  
Project Officer

//MARY LOU ROBINSON//

---

MARY LOU ROBINSON, DR-IV  
Chief, High Power Electromagnetics Division

This report is published in the interest of scientific and technical information exchange, and its publication does not constitute the Government's approval or disapproval of its ideas or findings.

# REPORT DOCUMENTATION PAGE

*Form Approved*  
OMB No. 0704-0188

Public reporting burden for this collection of information is estimated to average 1 hour per response, including the time for reviewing instructions, searching existing data sources, gathering and maintaining the data needed, and completing and reviewing this collection of information. Send comments regarding this burden estimate or any other aspect of this collection of information, including suggestions for reducing this burden to Department of Defense, Washington Headquarters Services, Directorate for Information Operations and Reports (0704-0188), 1215 Jefferson Davis Highway, Suite 1204, Arlington, VA 22202-4302. Respondents should be aware that notwithstanding any other provision of law, no person shall be subject to any penalty for failing to comply with a collection of information if it does not display a currently valid OMB control number. **PLEASE DO NOT RETURN YOUR FORM TO THE ABOVE ADDRESS.**

<b>1. REPORT DATE (DD-MM-YYYY)</b> 30-10-2015		<b>2. REPORT TYPE</b> Final		<b>3. DATES COVERED (From - To)</b> 30-09-2014 - 30-09-2015	
<b>4. TITLE AND SUBTITLE</b> Traveling Wave Amplifier Driven by a Large Diameter Annular Electron Beam in a Disk-Loaded Structure				<b>5a. CONTRACT NUMBER</b>	
				<b>5b. GRANT NUMBER</b> FA9451-14-1-0374	
				<b>5c. PROGRAM ELEMENT NUMBER</b> 62605F	
<b>6. AUTHOR(S)</b>  Yue Ying Lau				<b>5d. PROJECT NUMBER</b> 4867	
				<b>5e. TASK NUMBER</b> HD	
				<b>5f. WORK UNIT NUMBER</b> D07D	
<b>7. PERFORMING ORGANIZATION NAME(S) AND ADDRESS(ES)</b>  University of Michigan Department of Nuclear Engineering and Radiological Sciences 2355 Bonisteel Blvd. Ann Arbor, MI 48109-2104				<b>8. PERFORMING ORGANIZATION REPORT NUMBER</b>	
<b>9. SPONSORING / MONITORING AGENCY NAME(S) AND ADDRESS(ES)</b>  Air Force Research Laboratory 3550 Aberdeen Avenue SE Kirtland AFB, NM 87117-5776				<b>10. SPONSOR/MONITOR'S ACRONYM(S)</b>  AFRL/RDHP	
				<b>11. SPONSOR/MONITOR'S REPORT NUMBER(S)</b>  AFRL-RD-PS-TR-2015-0041	
<b>12. DISTRIBUTION / AVAILABILITY STATEMENT</b> Approved for public release: distribution unlimited.					
<b>13. SUPPLEMENTARY NOTES</b> OPS-15-9244					
<b>14. ABSTRACT</b> This project studies the viability of a high-power traveling wave tube (TWT) using a novel disk-on-rod slow-wave structure (SWS), which admits a large diameter, high current, annular electron beam. The annular electron beam carries a much higher current than a pencil beam, and the use of SWS allows moderate bandwidth. The gain and bandwidth were studied using analytic theory and simulation. The cold-tube as well as the hot-tube dispersion relation were constructed, from which the Pierce gain parameter, C, and the space charge parameter, QC, are extracted. Two very different methods were used to validate the calculation of C and they yield identical results. The gain was then calculated using Pierce classical theory of TWT based on C and QC, and was spot-checked against simulation results from the ICEPIC, MAGIC and CHRISTINE codes. Fair agreement was observed. The preliminary conclusion is that the disk-on-rod TWT is a viable, high-power extension to the conventional TWT which uses a pencil beam. The most important issue appears to be the excitation of unwanted modes.					
<b>15. SUBJECT TERMS</b> Traveling Wave Tube, High Power Microwaves					
<b>16. SECURITY CLASSIFICATION OF:</b>			<b>17. LIMITATION OF ABSTRACT</b>  SAR	<b>18. NUMBER OF PAGES</b>  20	<b>19a. NAME OF RESPONSIBLE PERSON</b> Matthew Domonkos
<b>a. REPORT</b> Unclassified	<b>b. ABSTRACT</b> Unclassified	<b>c. THIS PAGE</b> Unclassified			<b>19b. TELEPHONE NUMBER (include area code)</b>

Standard Form 298 (Rev. 8-98)  
Prescribed by ANSI Std. Z39.18

This page intentionally left blank.

# TABLE OF CONTENTS

Section	Page
List of Figures .....	v
List of Tables .....	vi
1.0 SUMMARY.....	1
2.0 INTRODUCTION .....	1
3.0 METHODS, ASSUMPTIONS AND PROCEDURES.....	2
3.1 Cold-Tube Dispersion Relation .....	2
3.2 Hot-Tube Dispersion Relation .....	5
3.3 Pierce's Parameters $C$ and $QC$ .....	6
4.0 RESULTS AND DISCUSSION .....	7
5.0 CONCLUSIONS.....	10
6.0 REFERENCES .....	11

## LIST OF FIGURES

<b>Figure</b>		<b>Page</b>
1	Schematic Diagram of the Disk-on-Rod TWT .....	2
2	Plots of the Fundamental Circuit Mode of the Cold-Tube Dispersion Relation (blue) and the Beam Mode (red). .....	4
3	Comparison of the Analytic Model of the Cold-Tube Dispersion Relation (blue) to Simulations in HFSS (green) for One Period.....	5
4	Spatial Amplification Rate as a Function of Beam Current Assuming $QC = 0$ (black) and Including $QC \neq 0$ (red).....	8
5	Plot of the Spatial Amplification Rate as a Function of DC Beam Current for the Operating Parameters in Tables 1 and 2, using Analytic Theory, ICEPIC, MAGIC, and CHRISTINE.....	9
6	Plot of the Imaginary Part of the Propagation Constant as a Function of Frequency for the Three Forward Waves in the Pierce 3-Wave Theory.....	10

## LIST OF TABLES

<b>Table</b>		<b>Page</b>
1	Dimensions for the Disk-on-Rod TWT for a Test Case. ....	3
2	Operating Parameters for a Test Case of the Disk-on-Rod TWT. ....	4
3	Tabulation of the Perveance [ $\mu\text{P}$ ], $C$ , and $4QC$ for Varying Beam Current $I$ . ....	7

This page intentionally left blank.



## 1.0 SUMMARY

There are many potential and present applications for high power microwave (HPM) devices, including electronic warfare, imaging, etc. For such coherent radiation sources, both high power output and wide bandwidth are required. However, the most studied HPM devices in the last 30 years, the relativistic klystron and the relativistic magnetron, are intrinsically narrow-band devices. Considered here is a new device, a traveling-wave tube (TWT) driven by a large-diameter annular electron beam in a Disk-on-Rod slow-wave structure (SWS). This device potentially offers wide bandwidth and high power and this research investigates its viability. In particular, the traditional TWT metrics, such as Pierce's gain parameter  $C$  and the space-charge parameter  $QC$  were derived so that comparisons may be made with currently operating TWTs. The cold-tube and hot-tube dispersion relations were also derived. The cold-tube dispersion relation compared favorably well with simulations using the simulation code HFSS. The hot-tube solution yielded the Pierce parameters  $C$  and  $QC$ . These parameters were used to calculate the gain according to Pierce's classical theory of TWTs, which was then spot-checked against three simulation codes, ICEPIC, MAGIC, and CHRISTINE. Fair agreement was found. The preliminary conclusion is that the Disk-on-Rod TWT is a viable, high power extension to the conventional TWT which uses a pencil beam. New issues of harmonic generation, proper accounting of  $QC$ , and TWT stability are identified.

## 2.0 INTRODUCTION

At the present, there are few high power amplifiers with wide bandwidth capability. The most studied HPM devices in the last 30 years, the relativistic klystron [1] and the relativistic magnetron [2], are intrinsically narrow-band devices [3]. Here we examine the alternative of a traveling-wave tube configuration in the multi-kA, 100 kV range. The amplifier configuration that is the focus of this research can potentially provide much higher power outputs than current high power commercial microwave amplification tubes while still maintaining the large bandwidths required by modern communications and state-of-the-art radar systems.

Instead of the traditional pencil beam, we will use a large-diameter relativistic annular electron beam for the Disk-on-Rod TWT (Fig. 1). A Disk-on-Rod slow-wave structure (SWS) will be used to provide wide bandwidth. It is placed coaxially with the annular beam and the outer wall of the TWT, which is a cylindrical metallic waveguide. Because of the increased cathode surface area for an annular beam, this large-diameter relativistic annular electron beam and SWS will have a much higher limiting current than a pencil beam. It is this combination of annular beam and SWS that provides both high power output and wide bandwidth.

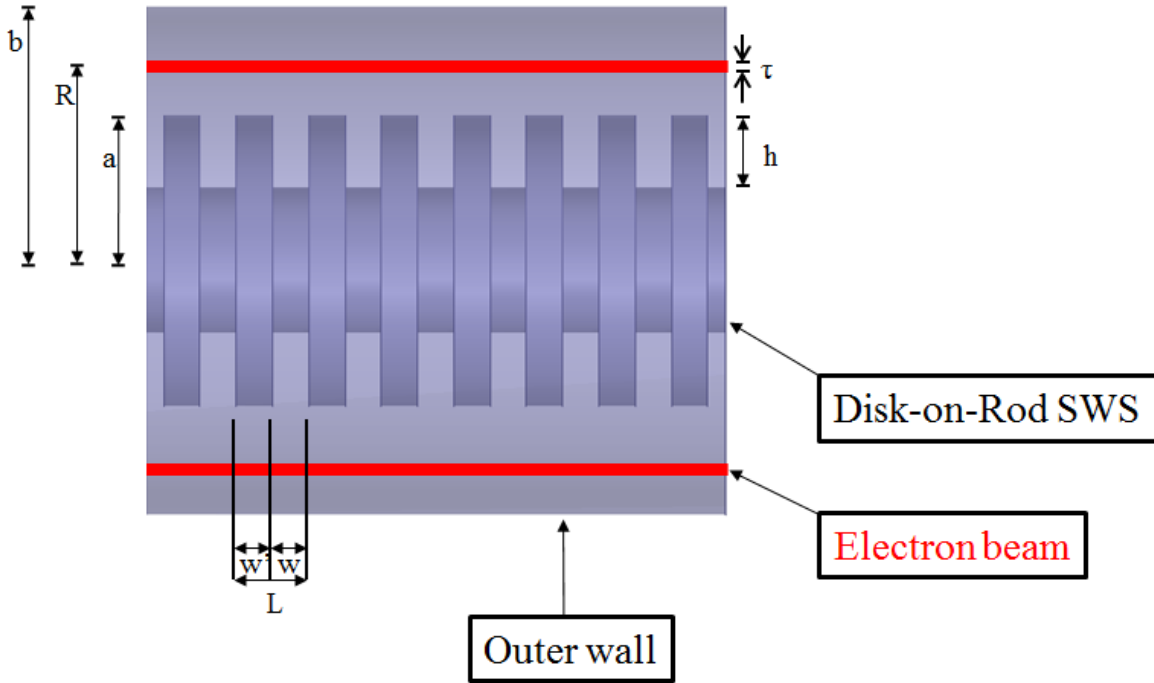


Figure 1. Schematic diagram of the Disk-on-Rod TWT

### 3.0 METHODS, ASSUMPTIONS, AND PROCEDURES

To evaluate the gain and bandwidth of a TWT, the most natural place to start is to use Pierce's classical TWT theory [4], and the Disk-on-Rod TWT is no exception [5]. Since we are facing a rarely studied device, this involves several steps: (a) the derivation of the cold-tube dispersion relation, (b) the construction of the hot-tube solution, (c) the extraction of Pierce's gain parameter  $C$  and space-charge parameter  $QC$  from the hot-tube solution and usage of them to evaluate the small signal gain from Pierce's standard 3-wave theory, and (d) the comparison of the analytic theory with simulation code results.

#### 3.1 Cold-Tube Dispersion Relation

To characterize the electromagnetic property of the SWS, the electron beam is removed. We consider transverse-magnetic (TM) electromagnetic waves in regions outside of the vanes and assume transverse electric and magnetic (TEM) waves in the cavities. Inhomogeneous wave equations for the magnetic and electric fields (decoupled) can be derived from combining Maxwell's Equations. Assuming  $e^{j\omega t - j\beta_n z}$  (harmonic) dependence for the fields and employing the Floquet Theorem for periodic structures, the equations for the fields are derived [6,7]. We next apply the appropriate boundary conditions: (1) tangential electric field must be zero at  $r = a - h$ , (2) tangential electric field must be continuous at  $r = a$ , (3) the spatially-averaged (across the cavity opening) magnetic field must be continuous at  $r = a$ , and (4) the electric field must be zero at  $r = b$ . With some algebra, the field equations are rearranged to give the cold-tube dispersion relation of the form [6,7]:

$$G(\omega, \beta_0) = \frac{U'(\frac{\omega a}{c})}{\frac{\omega}{c}U(\frac{\omega a}{c})} - \sum_{n=-\infty}^{\infty} \frac{(\sin \theta_n)^2}{\theta_n' \theta_n} \cdot \frac{V'(p_n a)}{p_n V(p_n a)} \equiv 0, \quad (1)$$

where

$$\beta_n = \beta_0 + \frac{2\pi n}{L}, \quad (2)$$

$$\theta_n = \frac{\beta_n w}{2}, \quad \theta_n' = \frac{\beta_n L}{2}, \quad (3)$$

$$p_n = \sqrt{\beta_n^2 - \frac{\omega^2}{c^2}}, \quad (4)$$

$$U\left(\frac{\omega r}{c}\right) = J_0\left(\frac{\omega(a-h)}{c}\right)Y_0\left(\frac{\omega r}{c}\right) - J_0\left(\frac{\omega r}{c}\right)Y_0\left(\frac{\omega(a-h)}{c}\right), \quad (5)$$

$$U'\left(\frac{\omega r}{c}\right) = J_0\left(\frac{\omega(a-h)}{c}\right)Y_1\left(\frac{\omega r}{c}\right) - J_1\left(\frac{\omega r}{c}\right)Y_0\left(\frac{\omega(a-h)}{c}\right), \quad (6)$$

$$V(p_n r) = I_0(p_n r)K_0(p_n b) - I_0(p_n b)K_0(p_n r). \quad (7)$$

We may rearrange this cold-tube dispersion relation into a more familiar form [6,7]:

$$\rightarrow \omega^2 - \omega_c^2(\beta_0) = 0, \quad (8)$$

where  $\omega_c(\beta_0)$  is the cold-tube circuit (angular) frequency as a function of the propagation constant of the fundamental circuit mode.

This dispersion relation is next plotted. The fundamental circuit mode along with the beam line for the test case are shown in Figure 2. The parameters used for the test case are listed in Tables 1 and 2.

**Table 1. Dimensions for the Disk-on-Rod TWT for a Test Case**

Dimensions [cm]	
b	3.5
R	2.8
a	2.3
h	1.3
w'	0.3
w	0.3
$\tau$	0.1

**Table 2. Operating Parameters for a Test Case of the Disk-on-Rod TWT**

Operating Parameters	
V [kV]	124
$\beta_{01}$ [ $\text{m}^{-1}$ ]	100
$f_{01}$ [GHz]	2.832

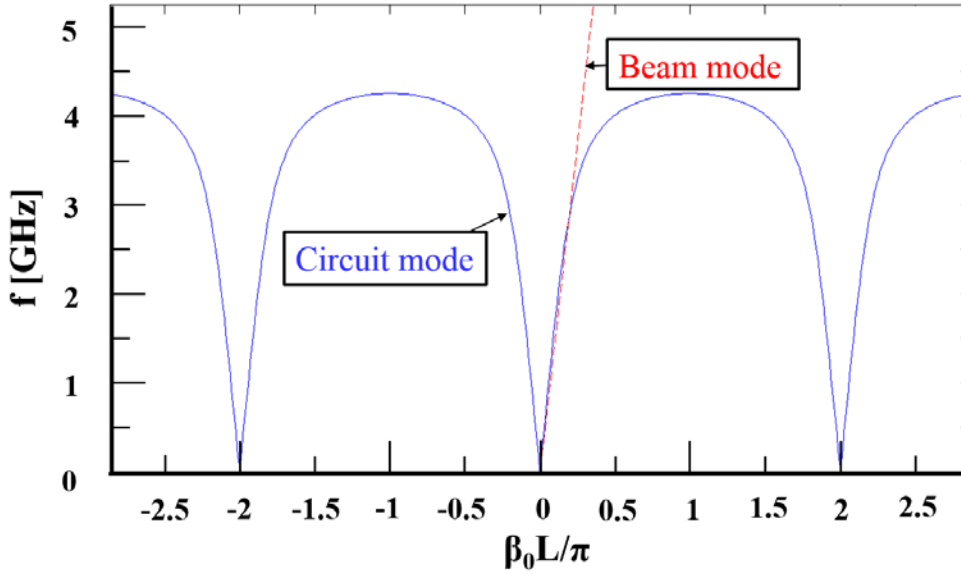


**Figure 2. Plots of the Fundamental Circuit Mode of the Cold-Tube Dispersion Relation (blue) and the Beam Mode (red)**

To validate the dispersion relation, (Eq. (1)) or (Eq. (8)), we designed the Disk-on-Rod TWT in the program High Frequency Structural Simulator (HFSS, [8]) and ran simulations to determine the eigen-frequencies. Shown in Figure 3 are the plots of the results from HFSS compared to the analytic theory. As can be seen, the HFSS simulations agree well with the analytic theory.

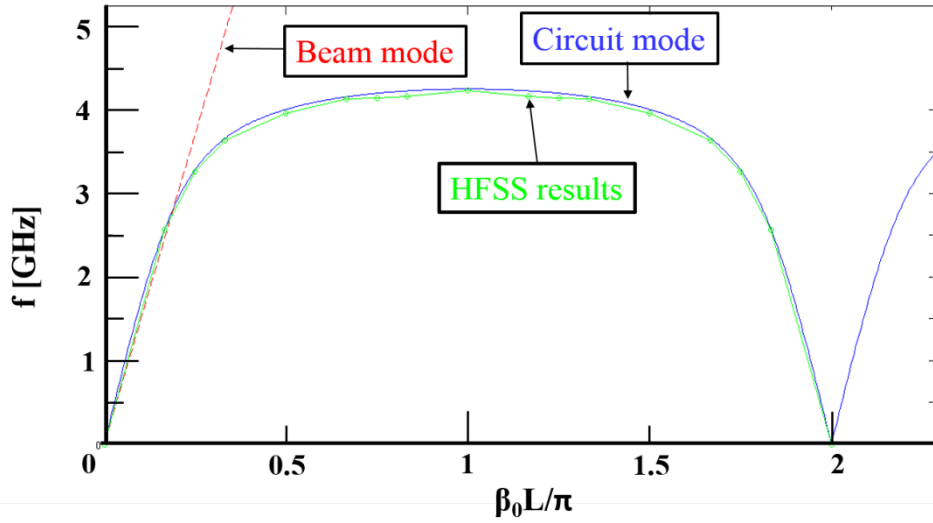


**Figure 3. Comparison of the Analytic Model of the Cold-Tube Dispersion Relation (blue) to Simulations in HFSS (green) for One Period**

### 3.2 Hot-Tube Dispersion Relation

We next derive the hot-tube dispersion relation including the annular electron beam using the technique given by Lau and Chernin [7]. The four boundary conditions given in Section 3.1 still hold, but we now add two more to account for the electron beam: (5) the tangential electric field must be continuous at the location of the beam ( $r = R$ ) and (6) the normal electric field suffers a discontinuity ( $\frac{\sigma_n}{\epsilon_0}$ , where  $\sigma_n$  is the surface charge density of the electron beam and  $\epsilon_0$  is the permittivity of free space) at  $r = R$ . It can be shown that the hot-tube dispersion relation takes the form:

$$D(\omega, \beta_n) \equiv \frac{U'(\frac{\omega a}{c})}{\frac{\omega}{c} U(\frac{\omega a}{c})} - \sum_{n=-\infty}^{\infty} \frac{(\sin \theta_n)^2}{\theta_n' \theta_n} \cdot \left\{ \frac{\omega_p^2 \tau}{(\omega - \beta_n v_0)^2 - p_n^2 \omega_p^2 \tau R \frac{V(p_n R)}{V(p_n a)} W_n} \cdot \frac{R}{a} \cdot \left( \frac{V(p_n R)}{V(p_n a)} \right)^2 + \frac{V'(p_n a)}{p_n V(p_n a)} \right\} = 0 \quad (9)$$

where

$$W_n = I_0(p_n R) K_0(p_n a) - I_0(p_n a) K_0(p_n R). \quad (10)$$

$v_0$  is the unperturbed electron drift velocity and  $\omega_p$  is the beam plasma frequency. It should be noted that  $\omega_p^2 \propto n_0$  (unperturbed electron number density)  $\propto I$  (DC beam current). If we remove the beam (i.e.  $I \propto n_0 \propto \omega_p^2 \rightarrow 0$ ), the above hot-tube dispersion relation collapses to the cold-tube dispersion relation, as expected.

The rather complicated hot-tube dispersion relation is to be casted into the standard Pierce theory [4,6], by extracting the gain parameter  $C$  and the space-charge parameter  $QC$ .

### 3.3 Pierce's Parameters $C$ and $QC$

Two of the most important parameters used by Pierce in his analysis of TWTs are: Pierce's gain parameter,  $C$ , and Pierce's AC Space-Charge Parameter  $QC$  [4,6,7].  $C$  (or  $C^3$ ) is a parameter that measures the coupling between the electron beam and the operating circuit mode. This parameter was calculated in two very different ways. In the first method, the coupling constant was extracted from an exact formulation of the space-charge wave on the SWS. We shall denote this by  $C$ . In the second method, the coupling constant was extracted from a consideration of the action of the beam on just the operating circuit mode. We shall denote this by  $C'$ . As seemingly different as these two methods (and hence values of the coupling constant) appear to be, the investigator's graduate student who has been supported by this grant, Patrick Wong, mathematically proved that *both of these methods yield identical results*. That is,  $C = C'$ .

The hot-tube dispersion relation (Eq. (9)) may be cast into the following form:

$$(\omega - \beta_0 v_0)^2 = \omega_p^2 \cdot R. \quad (11)$$

This is an *exact* equation, where  $R = R(\beta_0, \omega)$  is the plasma reduction factor. Let us decompose this plasma reduction factor into a singular part ( $R_S$ ) and the remainder ( $R_N$ ) [7]:

$$R = R_S + R_N. \quad (12)$$

The singular part ( $R_S$ ) is singular at the cold-tube circuit frequencies and essentially gives rise to the coupling constant. Hence, we may write:

$$R_S \propto \frac{\omega_p^2}{G(\omega, \beta_0)} = \frac{\omega_p^2}{\omega^2 - \omega_c^2} \propto \frac{C^3}{\omega^2 - \omega_c^2} \quad (13)$$

and upon substitution of this into (Eq.(11)) and ignoring the remainder, we get [7]:

$$(\omega - \beta_0 v_0)^2 \cdot (\omega^2 - \omega_c^2) \approx \omega^4 C^3, \quad (14)$$

which is Pierce's dispersion relation to lowest order. The term  $(\omega - \beta_0 v_0)$  is the beam mode, and the term  $(\omega^2 - \omega_c^2)$  is the circuit mode. The product of these two modes gives us a term that is proportional to  $C^3$ .  $C$  is extracted from an exact formulation of the space-charge wave on the SWS.

Alternatively, we derive  $C$  (now called  $C'$ ) from the action of the beam on just the operating circuit mode. We again begin with the inhomogeneous wave equation for the magnetic field obtained from combining and decoupling Maxwell's Equations,

$$\left[ \nabla^2 - \frac{1}{c^2} \frac{\partial^2}{\partial t^2} \right] \vec{H} = -\nabla \times \vec{J}. \quad (15)$$

Taking the inner product of this equation with  $\vec{H}^*$  (the complex conjugate of the magnetic field  $\vec{H}$ ), approximating the field with the vacuum field:  $\vec{H} \approx \vec{H}_v$ , and using the corresponding equation for the vacuum fields:  $\nabla^2 \vec{H}_v = -\frac{\omega_c^2}{c^2} \vec{H}_v$  (Helmholtz equation), we may derive an equation of the form [7]:

$$\omega^2 - \omega_c^2 = \frac{\iiint \vec{J}_1(\vec{E}_1) \cdot \vec{E}_1^* dV}{U}, \quad (16)$$

where  $\vec{E}$  is the electric field,  $U$  is the normalized energy content, and the volume integral is taken over a period of the structure.

Equation (16) gives the modification of the cold-tube frequency  $\omega_c$  [cf. Eq. (8)] by the current modulation. If the integral in (16) is evaluated, we arrive at the following equation:

$$(\omega - \beta_0 v_0)^2 \cdot (\omega^2 - \omega_c^2) = \omega^4 C^{-3}, \quad (17)$$

which is also the Pierce's dispersion relation to lowest order, of the same form as Equation 14. Mr. Patrick Wong, the graduate student of the investigator, has rigorously proven that  $C^{-3} = C^{-3}$ .

While the singular part of the plasma reduction factor  $R_S$  in Equation (12) gave rise to the coupling constant  $C$ , the remainder of the plasma reduction factor  $R_N$  gives rise to  $QC$ . With knowledge of the coupling constant (and  $R_S$ ) from two different methods (above), we may now compute the remainder exactly. The *difference* gives the remainder, which in turn gives  $QC$ , known as Pierce's space-charge parameter. To our knowledge, this is the first time that  $QC$  has been calculated exactly for a complex SWS.

#### 4.0 RESULTS AND DISCUSSION

For the test case whose parameters are given in Tables 1 and 2, we varied the beam current and calculated the perveance,  $C$ , and  $4QC$ . Our results are tabulated below (Table 3).

**Table 3. Tabulation of the Perveance [ $\mu\text{P}$ ],  $C$ , and  $4QC$  for Varying Beam Current  $I$**

<b>I [A]</b>	<b>Perv. [<math>\mu\text{P}</math>]</b>	<b>C</b>	<b>4QC</b>
6.25	0.1434	0.0287	0.1408
25	0.5736	0.0456	0.2232
<b>50</b>	<b>1.1472</b>	<b>0.0574</b>	<b>0.2812</b>
100	2.2944	0.0723	0.3544
200	4.5888	0.0911	0.4468
300	6.8832	0.1043	0.5112

In Table 3, the current of 50 A is highlighted. For this case, the beam perveance, defined as  $I/V^{3/2}$ , is 1.15  $\mu\text{P}$ ,  $C$  is 0.057, and  $4QC$  is 0.2812; these values are comparable to current high-performance TWTs. This suggests that this high power Disk-on-Rod TWT has the potential to perform on-par with the well-studied, lower power TWTs.

Lastly, we plot the spatial amplification rate  $\beta_i$  as a function of beam current  $I$  (Figure 4).

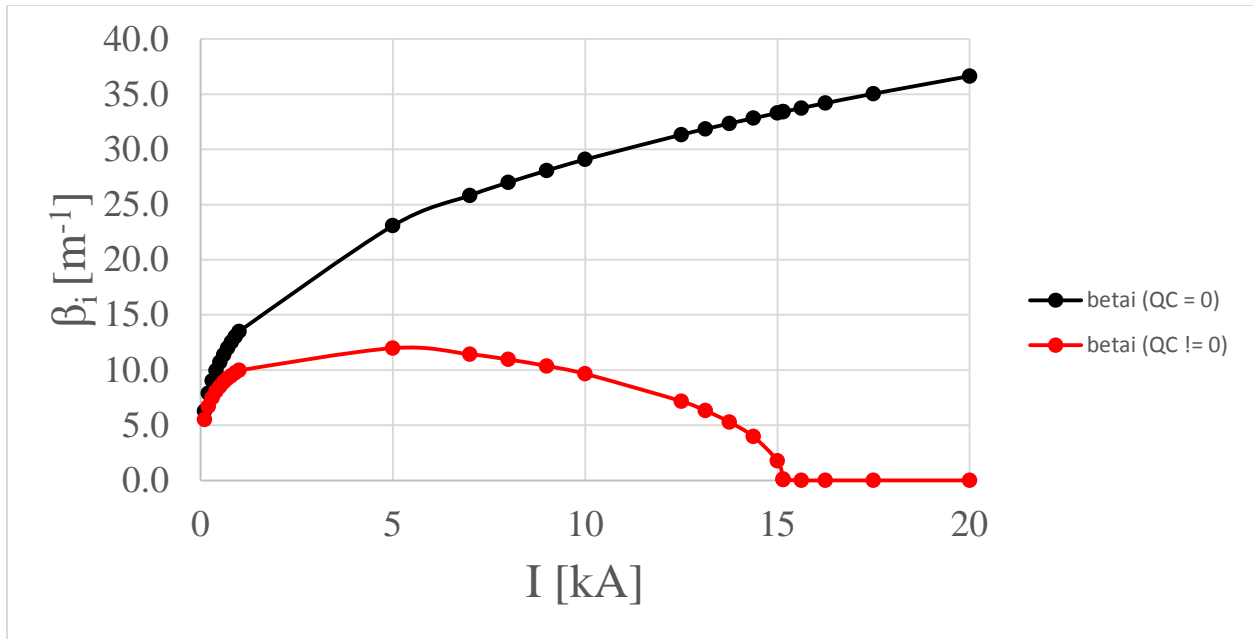


**Figure 4. Spatial Amplification Rate as a Function of Beam Current Assuming  $QC = 0$  (black) and Including  $QC \neq 0$  (red)**

As can be seen from Figure 4, when  $QC$  is set equal to zero (no space-charge effect, black curve), the gain is an approximation to the case when  $QC$  is nonzero (red curve) for low current but deviates significantly for higher current. There exists a critical current when  $QC$  is nonzero above which there is no further spatial amplification; this is a well-known effect in conventional TWTs. For our case, this critical current is about 15 kA.

The above analytic theory was compared with the results from the simulation codes ICEPIC [9] (ran by Dr. Brad Hoff of AFRL), MAGIC [10] (ran by graduate student David Simon of the University of Michigan), and CHRISTINE [11] (ran by Dr. David Chernin of Leidos Corporation) and are presented in Figure 5.



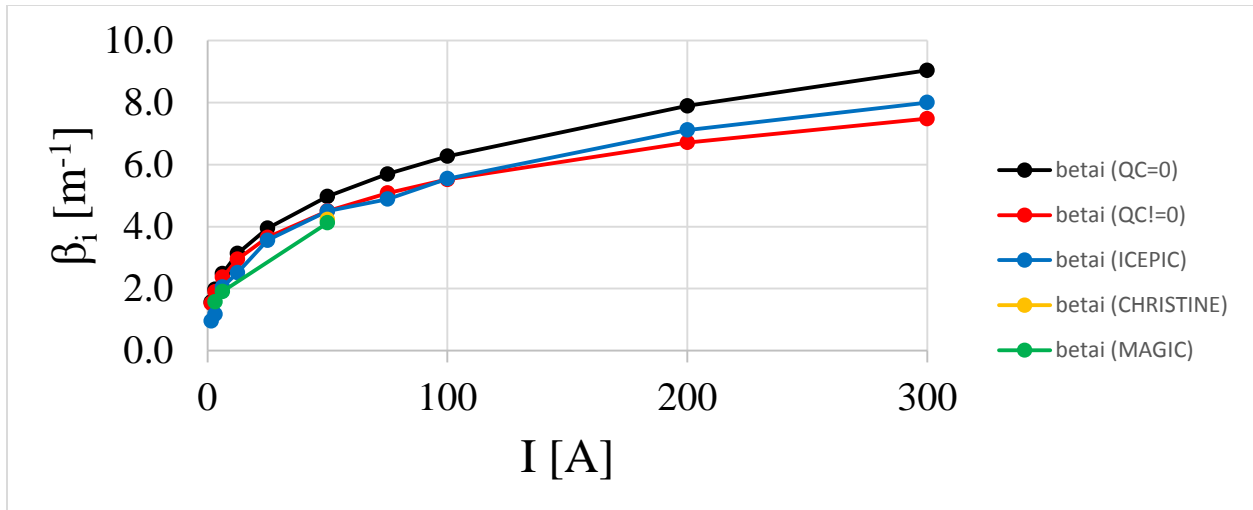


**Figure 5. Plot of the Spatial Amplification Rate as a Function of DC Beam Current for the Operating Parameters in Tables 1 and 2, using Analytic Theory, ICEPIC, MAGIC, and CHRISTINE**

According to Figure 5, there is general agreement between theory, ICEPIC, MAGIC, and CHRISTINE, validating to some extent not only the theory but the different simulation programs as well. The estimated RF power gain over an interaction length,  $L$ , is approximately given by  $\exp(2*\beta_i*L)$ . So it is to be cautioned that while there is general agreement in the spatial amplification rate ( $\beta_i$ ), there could be significant difference in the predicted RF output power.

Finally, the frequency dependence is examined. Figure 6 shows the imaginary part of the propagation constant (i.e. spatial amplification rate  $\beta_i$ ) of the three modes of Pierce in the hot-tube dispersion relation. Thus significant gain from the amplifying mode ( $\beta_i > 0$ ) can be obtained over a wide band of the Disk-on-Rod TWT.

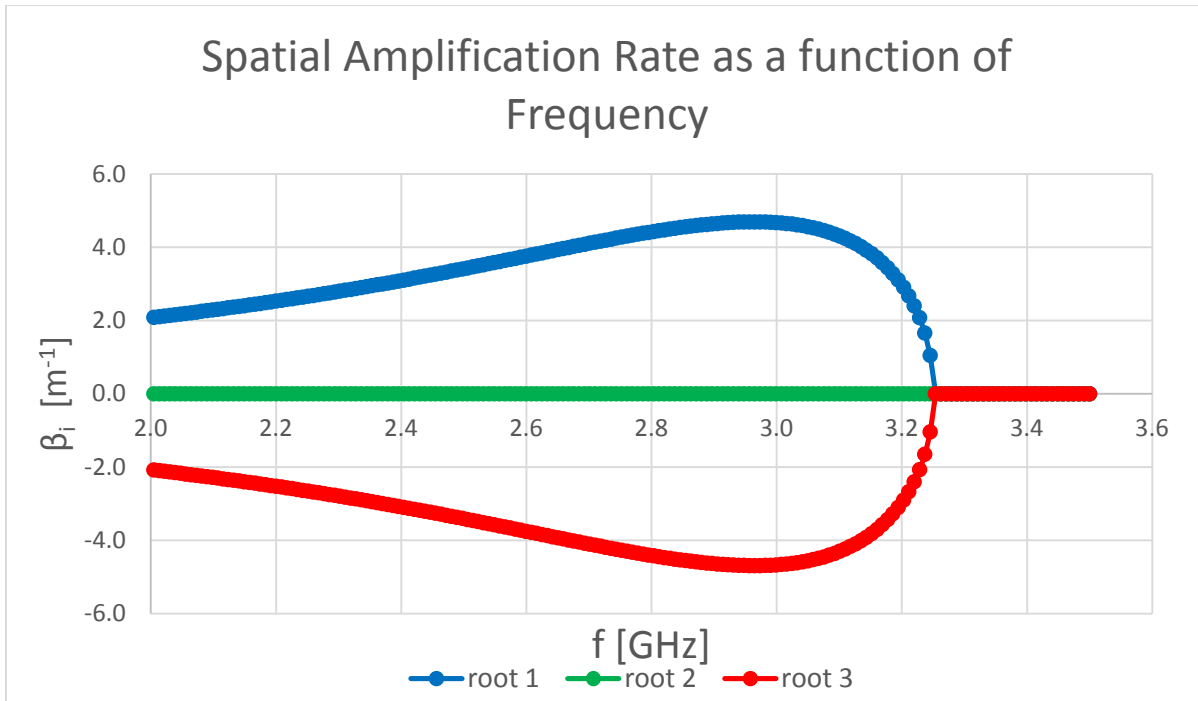


**Figure 6. Plot of the Imaginary Part of the Propagation Constant as a Function of Frequency for the Three Forward Waves in the Pierce 3-Wave Theory**

## 5.0 CONCLUSIONS

The Disk-on-Rod TWT was analyzed using the classical Pierce theory of TWTs. It does show the potential of high power and large bandwidth. These conclusions were corroborated by some preliminary simulations.

Several issues emerged from other studies which could be relevant to the Disk-on-Rod TWT.

(a) TWT oscillations. This is a generic problem in TWTs. The oscillations may be in the form of backward-wave oscillations, regenerative oscillations, and oscillations at the band-edge.

Oscillations at the band-edge was analyzed by the investigator recently [12]. Because the Disk-on-Rod TWT is overmoded, oscillations are the major concern.

(b) The issue of  $QC$ . Pierce's space-charge parameter is very important for a high current beam. How to evaluate it reliably in general remains an outstanding problem.

(c) Harmonic generation. Even in the linear regime, there could be significant harmonic content in the beam current due to crowding of an electron orbit [13]. It would be of interest to see if the Disk-on-Rod TWT can function as a bi-frequency amplifier.

## 6.0 REFERENCES

- [1] Luginsland, J.W., Lau, Y.Y., Hendricks, K.J., and Coleman, P.D., "A Model of Injection-Locked Relativistic Klystron Oscillator," *IEEE Trans. Plasma Sci.*, Vol. **24**, No. 3, pp. 935-937, 1996.
- [2] Nusinovich, G.S., Barker, R.J., Luhmann, N.C., and Booske, J.H., Modern Microwave and Millimeter-Wave Power Electronics, First Edition, Piscataway, NJ: Wiley-IEEE Press, 2005.
- [3] Benford, J., Swegle, J.A., and Schamiloglu, E., High Power Microwaves, Second Edition, Boca Raton, FL: CRC Press, 2007.
- [4] Pierce, J.R., Traveling-Wave Tubes, New York: Van Nostrand, 1950.
- [5] Field, L.M., "Some Slow-Wave Structures for Traveling-Wave Tubes," *Proc. IRE.*, Vol. **37**, No. 1, pp. 34-40, 1949; "Traveling wave tube," US Patent 2,645,737 (July 14, 1953).
- [6]ewartowski, G.W. and Watson, H.A., Principles of Electron Tubes, Princeton, NJ: Van Nostrand, 1966.
- [7] Lau, Y.Y. and Chernin, D., "A Review of the AC Space-Charge Effect in Electron-Circuit Interactions," *Phys. Fluids* **B4**, 3473-3497 (1992).
- [8] ANSYS HFSS, <http://www.ansys.com/Products/Electronics/ANSYS+HFSS>.
- [9] Peterkin, R.E., Jr. and Luginsland, J.W., "A virtual prototyping environment for directed-energy concepts," *Computing in Science & Engineering*, Vol. **4**, No. 2, pp. 42-49, 2002.
- [10] Goplen, B., Ludeking, L., Smith, D., and Warren, G., "User-configurable MAGIC for electromagnetic PIC calculations," *Comput. Phys. Commun.*, Vol. **87**, no. 1/2, pp. 54-86, 1995.
- [11] Antonsen, T.M. and Levush, B., "Traveling-Wave Tube Devices with Nonlinear Dielectric Elements," *IEEE Trans. Plasma Sci.*, Vol. **26**, No. 3, pp. 774-786, 1998.
- [12] Hung, D.M.H., Rittersdorf, I.M., Zhang, P., Chernin, D., Lau, Y.Y., Antonsen, T.M., Jr., Luginsland, J.W., Simon, D.H., and Gilgenbach, R.M., "Absolute instability near the band edge of traveling wave amplifiers," *Phys. Rev. Lett.* Vol. **115**, 124801 (2015).
- [13] Dong, C.F., Zhang, P., Chernin, D., Lau, Y.Y., Hoff, B., Simon, D.H., Wong, P., Greening, G., and Gilgenbach, R.M., "Harmonic content in the beam current in a traveling wave tube," *IEEE Trans. Electron Devices* (accepted, 2015).

## DISTRIBUTION LIST

DTIC/OCP

8725 John J. Kingman Rd, Suite 0944

Ft Belvoir, VA 22060-6218

1 cy

AFRL/RVIL

Kirtland AFB, NM 87117-5776

1 cy

Official Record Copy

AFRL/RDHP/Matthew Domonkos

1 cy